HHS Public Access

Author manuscript

Epilepsy Res. Author manuscript; available in PMC 2017 July 01.

Published in final edited form as:

Epilepsy Res. 2016 July ; 123: 20–28. doi:10.1016/j.eplepsyres.2016.04.001.

Low Functional Robustness in Mesial Temporal Lobe Epilepsy

C Garcia-Ramos[a], **J Song**[b], **BP Hermann**[c], and **V Prabhakaran**[a,c,d]

C Garcia-Ramos: garciaramos@wisc.edu; J Song: jie.z.song@gmail.com; BP Hermann: hermann@neurology.wisc.edu; V Prabhakaran: vprabhakaran@uwhealth.org

[a]Department of Medical Physics, University of Wisconsin School of Medicine and Public Health, 1111 Highland Ave. Rm 1005, Madison, WI, 53705-2275

[b]Biomedical Engineering, University of Wisconsin, College of Engineering, 1415 Engineering Drive, Madison, WI 53706

[c]Department of Neurology, University of Wisconsin School of Medicine and Public Health, Matthews Neuropsychology Lab, 7223 UW Medical Foundation Centennial Building, 1685 Highland Ave, Madison, WI 53705-2281

[d]Department of Radiology, University of Wisconsin School of Medicine and Public Health, E3/366 Clinical Science Center, 600 Highland Avenue, Madison, WI 53792-3252

Abstract

Objectives—Brain functional topology was investigated in patients with mesial temporal lobe epilepsy (mTLE) by means of graph theory measures in two differentially defined graphs. Measures of segregation, integration, and centrality were compared between subjects with mTLE and healthy controls (HC).

Methods—Eleven subjects with mTLE (age 36.5 ± 10.9 years) and 15 age-matched HC (age 36.8 ± 14.0 years) participated in this study. Both anatomically and functionally defined adjacency matrices were used to investigate the measures. Binary undirected graphs were constructed to study network segregation by calculating global clustering and modularity, and network integration by calculating local and global efficiency. Node degree and participation coefficient were also computed in order to investigate network hubs and their classification into provincial or connector hubs. Measures were investigated in a range of low to medium graph density.

Results—The group of patients presented lower global segregation than HC while showing higher global but lower local integration. They also failed to engage regions that comprise the default-mode network (DMN) as hubs such as bilateral medial frontal regions, PCC/precuneus complex, and right inferior parietal lobule, which were present in controls. Furthermore, the cerebellum in subjects with mTLE seemed to be playing a major role in the integration of their functional networks, which was evident through the engagement of cerebellar regions as connector hubs.

Corresponding author: Camille Garcia-Ramos, MS, Department of Medical Physics | School of Medicine and Public Health, 1111 Highland Ave, Rm 1005, Madison, WI 53705-2275, garciaramos@wisc.edu, Tel: (608) 262-2170, Fax: (608) 262-2413.

Conclusions—Functional networks in subjects with mTLE presented both global and local abnormalities compared to healthy subjects. Specifically, there was significant separation between groups, with lower global segregation and slightly higher global integration observed in patients. This could be indicative of a network that is working as a whole instead of in segregated or specialized communities, which could translate into a less robust network and more prone to disruption in the group with epilepsy. Furthermore, functional irregularities were also observed in the group of patients in terms of the engagement of cerebellar regions as hubs while failing to engage DMN-related areas as major hubs in the network. The use of two differentially defined graphs synergistically contributed to findings.

Keywords

Mesial Temporal Lobe Epilepsy; Resting-State fMRI; Graph Theory Analysis; Functional Hubs

1. Introduction

Mesial temporal lobe epilepsy (mTLE) is the most common localization-related epilepsy in the adult population (Engel et al, 1997). Disabling and medication resistant seizures, neurobehavioral comorbidities (cognitive and psychiatric complications), and reduced quality of life often accompany mTLE, making the surgical resection of the affected network a suitable option for this syndrome (Engel, 2003; Lachhwani et al, 2003; Lin et al, 2012). Although seizures occur in mesial temporal regions, which are important for the integrity of both semantic and episodic memory (McAndrews and Cohn, 2012), there is evidence that anatomical irregularities extend to other regions both ipsilateral and contralateral to the side of temporal lobe seizure onset, including the left thalamus, right middle cingulate gyrus, right thalamus, right and left postcentral gyrus, left precuneus, and the right precentral gyrus for left-hemispheric mTLE in terms of gray matter concentration (Holmes et al, 2013), which could help to explain the diffuse cognitive impairment that is often observed in this population (Doucet et al, 2013a; Hermann et al, 1997, Lin et al, 2012). Such diffuse impairment contributes to comprises in executive functions, language, and other abilities aside from the well-known memory-related deficits (Bell et al, 2011). In addition to cognitive dysfunction, behavioral and psychiatric comorbidities such as anxiety and depression are common as well (Doucet et al, 2013b; Quiske et al, 2000). Altogether, these neuropsychological and psychiatric disturbances indicate that mTLE is a disorder impacting not only functional systems arising from the anatomically affected area (e.g., memory), but also adversely affecting more global brain function (Zhao et al, 2014).

Recently, graph theoretical analyses have been implemented in brain networks at both the structural and functional levels and in both healthy and patient populations (Buckner et al, 2009; He et al, 2009a; for reviews: Bassett and Bullmore, 2009; He et al, 2009b). This has been possible since brain structure and function have been found to present complex graph-like properties such as integration and segregation. Having an integrated brain topology represents the capacity for effective communication and transfer of information, while segregation in the brain denotes the ability for specialized processes to take place. Aside from general network properties such as integration and segregation, centrality measures can be investigated in brain networks. Centrality is a property that investigates the influence of a

region inside a network, helping in the identification of the most crucial areas in the configuration of the network (Sporns et al, 2007).

Graph theory analyses have been implemented in mTLE patients at both the anatomical (Bernhardt et al, 2011; Bonilha et al, 2012; Liu et al, 2014) and functional (Doucet et al, 2014; Liao et al, 2010; Zhang et al, 2011) levels; however, for the functional studies, graph definitions have been mainly based on anatomical segmentation from structurally defined regions of interest (ROI) or nodes. The abstract nature of brain functional processes calls for a less strict network definition. Therefore in this study functional integrity in mTLE patients was studied with two differentially defined graphs: one using anatomically segmented nodes and the second one using nodes defined from putative functional networks. We believe that both forms would lead to a better understanding of brain function in a more complete manner by providing complementary information.

The main interest of this study is to investigate the resting-state functional networks in terms of integration and segregation in a sample of patients with mTLE. In addition, we wanted to investigate which functional regions were most important for functional communication by identifying the most central regions in the networks. Finally, we sought to determine how graph definition conveys differential information about functional brain topology.

2. Methods

2.1 Subjects

Eleven (age 36.5 ± 10.9 years) right-handed epilepsy patients with mesial temporal epilepsy were included in the study, along with fifteen (age 36.8 ± 14.0 years) age-matched healthy control subjects. Clinical characteristics for the patient group and summary of demographics for both groups can be found in Tables 1 and 2, respectively. Epilepsy participants were recruited from the University of Wisconsin (UW) clinical patient service while controls were recruited from the UW community. An MRI scan was acquired for each patient between August 2010 and August 2013 at the Health Emotions Research Institute (HERI) of the University of Wisconsin-Madison. Following the International League Against Epilepsy (Berg et al, 2010), diagnosis was based on clinical, EEG, and MRI characteristics. The University of Wisconsin Health Sciences Review Board approved all aspects of this study, and all participants provided voluntary written consent.

The patients of this study met the following criteria during clinical evaluation: (i) displayed one or more typical symptoms of mTLE and experienced complex partial seizures alone or accompanied by simple partial seizures and/or secondary generalized tonic-clonic seizures; (ii) MRI manifestations of the hippocampal sclerosis (HS) through unilateral hippocampal atrophy on T_1 image with associated hyperintensity on T_2 fluid attenuated inverted recovery image; (iii) no other structural MRI abnormality identified in the brain other than the hippocampal sclerosis.

2.2 Data Acquisition

During acquisition, all patients laid supine with their head securely held by straps and foam pads to minimize head motion. Participants were instructed to lie as still as possible with

their eyes closed, to not think of anything specific and to not fall asleep. Five-minute eyes-closed resting-state images were acquired using a 3.0-T MRI scanner (GE MRI 750, Milwaukee, USA) at the UW-Madison.

The eyes-closed resting-state functional MRI data on patients was acquired using an echo-planar imaging sequence with the following parameters: 28 axial slices, TR = 2.0 sec, TE = 30 ms, resolution/thickness = 3.5/5mm, FOV = 24 × 24 cm, 150 volumes. A high resolution (1 mm × 1 mm × 1mm) 3D T1-weighted BRAVO anatomical MRI was acquired in an axial orientation encompassing the entire brain. Functional data for healthy subjects was acquired from a research protocol with different acquisition parameters. The resting-state images were collected for 10 minutes with the following parameters: 42 slices, TR=2.6 sec, TE=22ms, isotropic 3.5mm, FOV=24 × 24cm, 231 volumes. A high resolution (1 mm × 1 mm × 1mm) 3D T1-weighted BRAVO anatomical MRI was acquired in an axial orientation encompassing the entire brain.

Differences in scanning parameters between groups are attributable to the different nature of recruitment from each group. Patients were recruited from the UW clinics, which have specific clinical parameters while healthy participants were recruited for participation in a clinically-independent research protocol. Such differences in acquisition have been found to affect in a negligible way seed-based functional connectivity matrices obtained from resting fMRI data, provided the same preprocessing steps (Gohel, 2009). Furthermore, in this study we used robust node-specific measures for the graph theory analysis to derive summary measures that are well-removed from the data acquisition parameters (Niu et al, 2013; Wang et al, 2011), which might further provide reliability of our results.

2.3 Preprocessing

Of the 11 mTLE patients, 3 had right mTLE and 8 had left mTLE. To increase the power of the analysis and to be able to refer to results as ipsilateral or contralateral MTLE, images for subjects with right mTLE were flipped from right to left (Blumenfeld et al, 2009; Zeng et al, 2013). Afterwards, preprocessing and analysis followed similarly for all subjects.

All preprocessing was done using the Analysis of Functional NeuroImages (AFNI) software (afni.nimh.nih.gov/afni/). The first five volumes from the acquisition were removed to account for scanner T1 steady state delay and for subjects to get used to the scanning environment. All images were then corrected for slice timing differences due to interleaved acquisition, and realigned to correct for head motion between volumes. Images were next spatially normalized to Talairach coordinates, resampled to isotropic 2mm, and smoothed to 4mm full-width half maximum (FWHM) Gaussian Kernel. CSF and WM signal were regressed out along with the six motion parameters (x, y, z, pitch, roll, yaw). Then, a temporal band-pass filter was applied (0.01 Hz < f < 0.1 Hz).

2.4 Creation of ROIs and Adjacency Matrices

The majority of studies implementing graph theory on functional scans use anatomical segmentation templates for the definition of ROIs or nodes. However, how graph theory metrics might differ between groups with differentially defined graphs might provide different/complementary information with which to further understand neurofunctional

configuration in patients with MTLE. Therefore, in this study, graph theory metrics were obtained from two differentially defined sets of nodes. The first one was based on 102 anatomically defined ROIs comprising cortical, subcortical, and cerebellar regions following Talairach segmentation (*TT_Daemon* template). The other was based on putative functional areas that belong to well-defined functional networks suggested by Power et al. (2011). They proposed a set of nodes based on regions that were activated in healthy individuals ($n > 300$) by tasks targeting different well-known systems. They ultimately proposed the use of 264 ROIs from which they provided their MNI coordinates for further use.

We included 235 from the 264 ROIs proposed by Power et al. (2011) that included nodes from the somatomotor, auditory, visual, cingulo-opercular task control, fronto-parietal task control, ventral attention, dorsal attention, and salience systems, and default-mode network (DMN), in addition to subcortical and cerebellar regions. We only used functional ROIs from which the function is known or has been associated to known functions (e.g., visual system, somatomotor system, etc.). The unused ROIs belong to systems that have not been clearly defined. Nodes were 4mm in radius. The MNI coordinates of the nodes used from Power et al (2011) can be found in the supplementary document.

Two adjacency matrices based on those two differentially defined sets of nodes were created for each subject using the *AFNI* program *ROI_Corr_Mat*. This program finds the Pearson correlation between each node, N and outputs it in an N x N matrix.

Graph theoretical measures were obtained using the Matlab-based Brain Connectivity Toolbox (BCT, http://www.brain-connectivity-toolbox.net/). Binary adjacency matrices were created to obtain different graph theory metrics. Measures obtained from the binary undirected graphs were calculated over a range of network cost or density. The density of a network constitutes the number of edges or connections that are used to constitute the system. In a network of N number of nodes, the total possible number of edges or connections would be $N(N-1)/2$, which means that for a network of 102 nodes, a density of 10% would represent 515 edges out of the 5,151 possible connections in the fully connected network. Given that brain networks have evolved to negotiate an economical trade-off between low cost and high topological value (Bullmore and Sporns, 2012), we investigated global measures in a range of low to medium density (5 to 40%) in 5% steps while node-specific measures such as local efficiency and network hubs were investigated at a density that represented full graph connectedness.

2.5 Graph measures

In this study measures of integration, segregation, and centrality were investigated between patients with mTLE and healthy controls. In order to explore graph integration, both global and local efficiency were calculated. The global efficiency of a graph was defined as the average of the inverse of each of the shortest paths (shorter routes of communication between nodes) in the network (Wang et al, 2010). Therefore, high global efficiency represents high integration of communication in the network. The local efficiency instead investigates the efficiency of communication between the neighbors of a node (Wang et al, 2010). See the appendix for more details.

Regarding graph segregation, measures of global clustering and modularity were investigated. Global clustering or transitivity is the ratio of “triangles” (closed connection between three nodes) to “triplets” (connections between three nodes) in the network (Humphries and Gurney, 2008; Newman, 2003). Therefore, it lies between 0 and 1, with 1 indicating a fully clustered network. This is a measure that reflects how clustered or segregated a network is. The modularity of a network is the configuration of such network into segregated communities that contribute to the same processes. Unlike the other measures, modularity is statistically estimated instead of computed exactly (Blondel et al, 2008). The modularity index is a measure of the goodness of the subdivision of the graph into communities; the higher it is, the strongest the modular structure of the graph (Boccalletti et al, 2006). Modularity in a functional network is of great importance because it not only allows for specialized processes to happen but also provides functional containment of community perturbations that would be easily spread to the rest of the network otherwise; therefore it is a measure of network robustness (Kitano, 2004). Since the number of modules might vary with different iterations, modularity should be calculated more than once in order to know the most likely number of modules in each graph. For this work, it would be calculated 100 times per graph. The Force Atlas algorithm of the open source software *Gephi* (http://gephi.github.io/) was used for the 2D visualization of modularity on each group (attraction strength=10, repulsion strength=200, gravity=30).

In order to investigate the network hubs, which are the most fundamental regions for the configuration of a network (Sporns et al, 2007), the node degree was the centrality measure used to investigate them. The degree of a node is the sum of the edges or connections that a given node has. Nodes with high degree (> average + SD) would be considered hubs of the network. Hubs can be defined as provincial hubs, which are the ones having most of the connections within their own module, or connector hubs, which are the ones that connect mainly to nodes from different modules (Sporns et al, 2007). The participation coefficient (PC) of a node conveys information about which of the nodes connections are intermodular; it tends to 1 if it’s mainly connected to other modules and is 0 if it has no intermodular connections. Nodes with high degree and high participation coefficient were considered connector hubs, while nodes with low PC but high degree were considered provincial hubs. The threshold for a node to be either connector or provincial hub was set to 60% of the maximum PC (Sporns et al, 2007). The maximum PC in a network depends on the number of modules in the network, according to this equation:

$$PC_i = 1 - \sum_{m=1}^{N_M} \left(\frac{\kappa_{im}}{k_i} \right)^2,$$

where k_i is the degree of node i, κ_{im} is the number of such degrees connected to module m, and N_M is the total number of modules in the graph.

3. Results

Graph theory metrics were investigated between patients with mesial temporal lobe epilepsy and healthy controls and no statistically significant differences were found between groups

in age (p=0.95) and gender (χ^2=2.75, df=1, p=0.13). Node-specific measures were calculated at 37%, which was the density level in which both groups presented no disconnected nodes in the graph. Two-sided t-tests were implemented to find significant statistical group differences at each density level. Bonferroni correction was implemented to correct for multiple comparisons when investigating global measures (8 density levels and 3 tests), and FDR (false discovery rate) correction was performed when investigating node-specific measures like local efficiency.

3.1 Global integration and segregation

Network integration was investigated by calculating global efficiency in both kinds of graphs. The group of subjects with mTLE presented slightly higher global efficiency than control subjects that was significant at low graph density only in the anatomically defined graph (Figure 1).

Global clustering was calculated to measure global segregation in each group. It monotonically increased with increasing connection density in both groups and for both kinds of graphs (Figure 2), with the functional network showing the most parallel change between groups (Figure 2, right). However, groups presented a marked separation across the range of density thresholds in which healthy controls were higher than the mTLE group, being statistically significant from low to medium density in the anatomically defined graph (Figure 2, left), but only at 40% in the functionally defined graph (Figure 2, right).

Regarding the modularity index (Figure 3), which was also obtained over a range of density thresholds, both groups presented similar values with no significant differences noted at any density threshold.

3.2 Local integration and segregation

Local integration was investigated at a density of 37% by calculating local efficiency between groups in both differentially defined graphs (Figure 4). The group of patients presented significantly lower local efficiency across most of the nodes in the frontal, parietal, temporal, and occipital lobes, cingulate cortex and insular regions in the anatomically defined graph while showing similar local efficiency over most subcortical and cerebellar regions when compared to controls. However, the group of patients presented significantly higher local efficiency in the right lateral globus pallidus (subcortical area) and the left inferior semilunar lobule (cerebellar region) when compared to controls. In the functionally defined graph, mTLE subjects showed significantly lower local efficiency over most nodes, specifically those representing the somatomotor, auditory, visual, task control, and attention systems, and some nodes of the default-mode network, subcortical regions, and cerebellar areas. None of the regions presented significantly higher local efficiency in the group of patients compared to controls.

When investigating the 2D visualization of the network (Figure 5), i.e., a way to have an overview of graph segregation and integration; in the anatomically defined graph, cerebellar regions (green module) were more integrated to the rest of the nodes in the patients while they were more segregated and less integrated to the rest of the network in the group of controls. Furthermore, the group of patients presented a module composed only of

subcortical regions (blue module) while subcortical regions in controls were integrated to the rest of the network, especially to frontal and insular regions (blue module). In the functionally defined graphs, differences were not as evident, although higher segregation was also appreciated in the graph of healthy controls.

3.3 Hubs of the network

In Figure 5, the network hubs were identified in the modular configuration of each group network in order to provide their role in the segregation of the graphs, however in Figure 6 the approximate anatomical location of the hubs in the brain can be appreciated along with their classification into provincial or connector hubs. In the anatomically defined network (Figure 6, top), hubs were mainly located in frontal, temporal, and cerebellar regions for the group of patients, while they were mostly located in frontal, parietal, and temporal regions in the group of controls. Furthermore, regarding regions commonly associated with the DMN, the control group presented bilateral medial frontal gyrus, bilateral inferior parietal lobule (IPL), right precuneus, and right posterior cingulate as hubs, while the group of patients only had the left IPL as a hub. Also, subjects with mTLE presented four cerebellar regions as connector hubs while controls presented two cerebellar regions as provincial hubs.

In the functionally defined graph (Figure 6, bottom) a great proportion of hubs were from the somatomotor system in controls, followed by some visual, auditory, and attention systems. However, in mTLE, hubs were more evenly distributed across the somatomotor, visual, attention, auditory, task control, and DMN systems. It is visually evident that hubs in patients were distributed across systems in the brain while they are more concentrated in sensorimotor systems in controls.

4. Discussion

In this study, graph theory measures of segregation, integration, and centrality were investigated in the resting-state networks of patients with mesial temporal lobe epilepsy and a group of age-matched controls for both structurally and functionally defined graphs. The main findings are as follows: (1) patients presented a slightly more integrated but significantly less segregated network than controls, which may be indicative of a less robust network in mTLE; (2) the mTLE group failed to engage the posterior cingulate cortex (PCC) and precuneus along with other DMN-related regions as network hubs while engaging cerebellar regions as hubs of network indicating abnormal reorganization; (3) local efficiency of frontal, parietal, temporal, and occipital regions seems affected in mTLE while local efficiency in subcortical and cerebellar regions seem less compromised; (4) both anatomically and functionally defined graphs contributed differentially to findings at the node level.

4.1 Network segregation and integration

In this study we showed that the mTLE group presented significantly lower global segregation – as represented by global clustering and the 2D visualization of modularity – while at the same time presenting slightly higher global integration – as represented by global efficiency – than the group of healthy controls, which is in accordance with previous

studies (Doucet et al., 2014; Song et al, 2015). The considerably lower global segregation observed in patients could translate into a network that lacks the capacity to contain functional processes into a specific community within the brain making it less specialized. The reduced capacity to engage in segregated communities could also expose the given module to disruptions from other communities in the brain. Also, due to high global integration the risk of spreading perturbations from epilepsy increases, which could be a factor contributing to cognitive disruptions such as executive function and language abilities typically observed in this group of patients (Bell et al, 2011) and that comprise functional regions far from the epilepsy site (i.e., mesial temporal region) in healthy participants (Fedorenko et al, 2011).

Interestingly, cerebellar regions were integrated to the rest of the network as a whole in the mTLE group while cerebellar regions were more *separated* from the rest of the modules in the network of controls. This abnormal integration of the cerebellum to the cerebrum in mTLE could represent an attempted adaptive or compensatory process in which the brain should *work together* to help maintain cognitive function. Some but not all prior studies have found that the cerebellum is positively involved in seizure inhibition (Cooper et al, 1973; Davis and Emmonds, 1992) as well as with a more favorable prognosis after temporal lobectomy (Specht et al, 1997). Also, cerebellar atrophy has been associated with disease severity (e.g. duration of epilepsy, and number of seizures across the lifetime) (Hermann et al, 2005) and lower procedural memory (Hermann et al, 2004) in patients with temporal lobe epilepsy. However, due to lack of cognitive/behavioral measures, investigations of neuropsychological significance of the higher cerebellar integration observed in the group of patients of this study could not be investigated rendering unfeasible any conclusions about possible compensatory mechanisms.

The group of patients presented significantly lower local efficiency over most regions of the cerebrum (Figure 5) while presenting with similar local efficiency than controls for most of subcortical and cerebellar regions. However, a subcortical region (right globus pallidus) and a cerebellar area (left lateral semilunar lobule) presented significantly higher local efficiency in the group of patients, therefore indicating higher interaction between the neighbors of these two nodes in the group of patients. Such lower local efficiency in the group with epilepsy could be beneficial since possible disruptions in a node might not necessarily affect nearby nodes. For example, this might be the reason why executive function or language processes are not entirely disrupted.

In summary, neuropsychological abilities of patients with mTLE might be affected as a consequence of the high global integration and low segregation that exists functionally, allowing the spread of perturbations more easily across the brain. This is a hypothesis that can be tested in the future.

4.2 Network Centrality

Network centrality was investigated through the calculation of the functional hubs in both patients and controls. Hubs in the network of the mTLE group were notably different from the hubs in control subjects. In the anatomically defined network, hubs were mainly located in frontal, temporal, and cerebellar regions for the group of patients, while they were mostly

located in frontal, temporal, and parietal regions in the group of controls. Furthermore, contrary to the mTLE group, the healthy subjects engaged the right PCC and precuneus along with bilateral medial frontal gyrus, and bilateral inferior parietal lobule (IPL) as connector hubs, which are important areas from the DMN (Buckner et al, 2009; Mevel et al, 2013; Persson et al, 2007). In this study, subjects with mTLE were not engaging the majority of the expected regions as main hubs, especially the PCC and precuneus, which coincides with previous publications that found disrupted DMN in mTLE patients (Coan et al, 2014; Liao et al., 2010; McCormick et al, 2013). Along with the lack of recruitment of most DMN-related regions as hubs, mTLE participants presented four regions from the cerebellum as connector hubs in the network while controls only presented two cerebellar regions only as provincial hubs. Functional connectivity studies have found that the cerebellum participates not just in motor function, but also attention, cognitive control, and default-mode systems (Buckner et al, 2011). Its involvement as connector hub in the group of patients could potentially represent an attempted adaptive process in which such cerebellar regions are taking over more of the load that traditionally corresponds to the cerebrum. However, the connection between involvement of cerebellar regions and the lack of engagement of most DMN-related regions as network hubs in the group of patients would be questions for future studies.

In summary, centrality seems adversely affected in the group of patients, with specific disruptions involving the parietal lobe and the cerebellum, which are areas involved in important neuropsychological processes such as language (Bernal et al, 2015), phonological decisions, numerical retrieval, attention (Humphreys and Lambon, 2015), and performance monitoring (Peterburs et al, 2015).

In this study we showed that different information can be obtained when using different nodes definition (i.e., based on anatomical segmentation or in functionally-based ROIs) but mainly regarding network hubs. Evidently, global properties such as clustering, harmonic mean, and modularity presented the same qualitative information regardless of the nodes definition with main differences regarding statistical significance, which might be attributed to power (small *n*). The differences obtained at the network hubs could be expected given the different nature of node location and size. For example, in the anatomically-defined nodes, the areas are bigger, therefore the averaging of functional correlation coefficient would be more diluted than in the functionally-defined graph where nodes comprised smaller cortical areas (4mm in radius) on average. Therefore, we could speculate that the functionally-defined graph could be more sensitive to capturing node-specific functional information (i.e., hubs) while the anatomically-defined graph would be enough when the study hypothesis is more centered around global graph information.

4.3 Limitations of the study

One of the limitations of this study is the relatively small sample size, which limited the power of the analysis. Graph theory metrics seem to be robust despite small sample size in previous studies (He et al, 2009a), however further graph theory analyses combining differentially defined graphs should be explored in larger samples. Another limitation is that only a few subjects could undergo neuropsychological evaluations; therefore, precluding any

conclusions about the nature of results –if compensatory or detrimental. In addition, the different scanning parameters must be considered. The mTLE group data was not acquired based on a research protocol like control subjects but based on clinical data obtained under the parameters of the clinic, the matching of scanning parameters such as repetition time, echo time, and voxel size between groups was not under our control. However, it has been demonstrated that different scanning parameters negligibly affects seed-based functional connectivity matrices obtained from resting fMRI data, like the ones in this study, as long as the pre-processing steps are the same (Gohel, 2009). Specifically, "the investigation demonstrated a strong correlation between cross-correlation values for pair of ROIs between sites. These findings suggest reliability and consistency of resting state brain networks between sites" (Gohel, 2009). Furthermore, a previous study from our group showed a high level of reliability of RSFC in normal healthy subjects with different voxel sizes (Song et al., 2012). Moreover, the graph theory metrics used to calculate node-specific measures (i.e., degree and local efficiency) have proven to be very robust regardless of physiological state (i.e., level of blood oxygenation; Niu et at, 2013) and specially if networks are binary (Wang et al, 2011); although those studies did not involve differences in scanning parameters. Therefore, even though different scanning parameters have proven to not affect seed-based connectivity matrices, and the chosen node-specific graph theory metrics are robust, the results from this study should be interpreted based on these limitations.

5. Conclusion

Patients with mesial temporal lobe epilepsy presented a less robust and specialized network compared to control participants. They seemed to be relying on more direct connections to support brain topology along with less segregated functional processes rendering a less modular topology possibly as a consequence of seizures. These patients also failed to engage DMN-related regions such as the PCC and precuneus complex, right IPL, and bilateral medial frontal gyrus as network hubs while recruiting bilateral cerebellar regions as major hubs of the network. The use of two differentially defined graphs synergistically contributed to findings at the local level and provided similar results at the global level. Whether these functional topological abnormalities found in patients represent an adaptive or compensatory process remain to be investigated.

Supplementary Material

Refer to Web version on PubMed Central for supplementary material.

Acknowledgments

The authors acknowledge the financial support of NIH grants NINDS 3R01NS044351-09S1, 1K23NS086852-01A1, and 1R01 NS081926-01. They also thank the medical student Joshua Suhonen for his collaboration in the study.

References

Bassett DS, Bullmore ET. Human brain networks in health and disease. Curr Opin Neurol. 2009; 22(4):340–347. [PubMed: 19494774]

Bell B, Lin JJ, Seidenberg M, Hermann B. The neurobiology of cognitive disorders in temporal lobe epilepsy. Nat Rev Neurol. 2011; 7(3):154–164. [PubMed: 21304484]

Berg AT, Berkovic SF, Brodie MJ, Buchhalter J, Cross JH, van Emde Boas W, Engel J, French J, Glauser TA, Mathern GW, Moshé SL, Nordli D, Plouin P, Scheffer IE. Revised terminology and concepts for organization of seizures and epilepsies: report of the ILAE Commission on Classification and Terminology, 2005–2009. Epilepsia. 2010; 51(4):676–685. [PubMed: 20196795]

Bernal B, Ardila A, Rosselli M. Broca's area network in language function: a pooling-data connectivity study. Front Psychol. 2015; 6:687. [PubMed: 26074842]

Bernhardt BC, Chen Z, He Y, Evans AC, Bernasconi N. Graph-theoretical analysis reveals disrupted small-world organization of cortical thickness correlation networks in temporal lobe epilepsy. Cereb Cortex. 2011; 21(9):2147–2157. [PubMed: 21330467]

Blondel VD, Guillaume J-L, Lambiotte R, Lefebvre E. Fast unfolding of communities in large networks. J Stat Mech. 2008:P10008.

Blumenfeld H, Varghese GI, Purcaro MJ, Motelow JE, Enev M, McNally KA, Levin AR, Hirsch LJ, Tikofsky R, Zubal IG, Paige AL, Spencer SS. Cortical and subcortical networks in human secondarily generalized tonic–clonic seizures. Brain. 2009; 132:999–1012. [PubMed: 19339252]

Boccaletti S, Latora V, Moreno Y, Chavez M, Hwang DU. Complex networks: Structure and dynamics. Phys Rep. 2006; 424:175–308.

Bonilha L, Nesland T, Martz GU, Joseph JE, Spampinato MV, Edwards JC, Tabesh A. Medial temporal lobe epilepsy is associated with neuronal fibre loss and paradoxical increase in structural connectivity of limbic structures. J Neurol Neurosurg Psychiatry. 2012; 83(9):903–909. [PubMed: 22764263]

Bullmore E, Sporns O. The economy of brain network organization. Nat Rev Neurosci. 2012; 13(5): 336–349. [PubMed: 22498897]

Buckner RL, Krienen FM, Castellanos A, Diaz JC, Yeo BT. The organization of the human cerebellum estimated by intrinsic functional connectivity. J Neurophysiol. 2011; 106(5):2322–2345. [PubMed: 21795627]

Buckner RL, Sepulcre J, Talukdar T, Krienen FM, Liu H, Hedden T, Andrews-Hanna JR, Sperling RA, Johnson KA. Cortical hubs revealed by intrinsic functional connectivity: mapping, assessment of stability, and relation to Alzheimer's disease. J Neurosci. 2009; 29(6):1860–1873. [PubMed: 19211893]

Coan AC, Campos BM, Beltramini GC, Yasuda CL, Covolan RJ, Cendes F. Distinct functional and structural MRI abnormalities in mesial temporal lobe epilepsy with and without hippocampal sclerosis. Epilepsia. 2014; 55(8):1187–1196. [PubMed: 24903633]

Cooper IS, Crighel E, Amin I. Clinical and physiological effects of stimulation of the paleocerebellum in humans. J Am Geriatr Soc. 1973; 21(1):40–43. [PubMed: 4682565]

Davis R, Emmonds SE. Cerebellar stimulation for seizure control: 17-year study. Stereotact Funct Neurosurg. 1992; 58(1–4):200–208. [PubMed: 1439341]

Doucet GE, Sharan A, Pustina D, Skidmore C, Sperling MR, Tracy JI. Early and Late Age of Seizure Onset have a Differential Impact on Brain Resting-State Organization in Temporal Lobe Epilepsy. Brain Topogr. 2014 Epub ahead of print.

Doucet G, Osipowicz K, Sharan A, Sperling MR, Tracy JI. Extratemporal functional connectivity impairments at rest are related to memory performance in mesial temporal epilepsy. Hum Brain Mapp. 2013a; 34(9):2202–2216. [PubMed: 22505284]

Doucet GE, Skidmore C, Sharan AD, Sperling MR, Tracy JI. Functional connectivity abnormalities vary by amygdala subdivision and are associated with psychiatric symptoms in unilateral temporal epilepsy. Brain Cogn. 2013b; 83(2):171–182. [PubMed: 24036129]

Engel, J., Jr; Williamson, PD.; Wieser, H-G. Mesial Temporal Lobe Epilepsy. In: Engel, J., Jr; Pedley, TA., editors. Epilepsy: a comprehensive textbook. Philadelphia: Lippincott-Raven; 1997. p. 2417-2426.

Engel J. A Greater Role for Surgical Treatment of Epilepsy: Why and When? Epilepsy Curr. 2003; 3(2):37–40. [PubMed: 15309078]

Fedorenko E, Behr MK, Kanwisher N. Functional specificity for high-level linguistic processing in the human brain. Proc Natl Acad Sci U S A. 2011; 108(39):16428–16433. [PubMed: 21885736]

Gohel, SR. Masters Thesis. New Jersey Institute of Technology; 2009. Reliability of resting brain networks using FMRI. Retrieved from http://library1.njit.edu/etd/2000s/2009/njit-etd2009-036/njit-etd2009-036.html

He Y, Wang J, Wang L, Chen ZJ, Yan C, Yang H, Tang H, Zhu C, Gong Q, Zang Y, Evans AC. Uncovering Intrinsic Modular Organization of Spontaneous Brain Activity in Humans. PLoS One. 2009a; 4(4):e5226. [PubMed: 19381298]

He Y, Chen Z, Gong G, Evans A. Neuronal Networks in Alzheimer's Disease. Neuroscientist. 2009b; 15(4):333–350. [PubMed: 19458383]

Hermann BP, Bayless K, Hansen R, Parrish J, Seidenberg M. Cerebellar atrophy in temporal lobe epilepsy. Epilepsy Behav. 2005; 7(2):279–287. [PubMed: 16051525]

Hermann B, Seidenberg M, Sears L, Hansen R, Bayless K, Rutecki P, Dow C. Cerebellar atrophy in temporal lobe epilepsy affects procedural memory. Neurology. 2004; 63(11):2129–2131. [PubMed: 15596761]

Hermann BP, Seidenberg M, Schoenfeld J, Davies K. Neuropsychological characteristics of the syndrome of mesial temporal lobe epilepsy. Arch Neurol. 1997; 54(4):369–376. [PubMed: 9109737]

Holmes MJ, Yang X, Landman BA, Ding Z, Kang H, Abou-Khalil B, Sonmezturk HH, Gore JC, Morgan VL. Functional networks in temporal-lobe epilepsy: a voxel-wise study of resting-state functional connectivity and gray-matter concentration. Brain Connect. 2013; 3(1):22–30. [PubMed: 23150897]

Humphreys GF, Lambon Ralph MA. Fusion and Fission of Cognitive Functions in the Human Parietal Cortex. Cereb Cortex. 2015; 25(10):3547–3560. [PubMed: 25205661]

Humphries MD, Gurney K. Network 'Small-World-Ness': A Quantitative Method for Determining Canonical Network Equivalence. PLoS ONE. 2008; 3(4):e2051.

Kitano H. Biological robustness. Nat Rev Genet. 2004; 5(11):826–837. [PubMed: 15520792]

Lachhwani R, Lüders H. In refractory temporal lobe epilepsy, consider surgery sooner. Cleve Clin J Med. 2003; 70(7):649–53. [PubMed: 12882388]

Liao W, Zhang Z, Pan Z, Mantini D, Ding J, Duan X, Luo C, Lu G, Chen H. Altered functional connectivity and small-world in mesial temporal lobe epilepsy. PLoS One. 2010; 5(1):e8525. [PubMed: 20072616]

Liu M, Chen Z, Beaulieu C, Gross DW. Disrupted anatomic white matter network in left mesial temporal lobe epilepsy. Epilepsia. 2014; 55(5):674–682. [PubMed: 24650167]

Lin JJ, Mula M, Hermann BP. Uncovering the neurobehavioural comorbidities of epilepsy over the lifespan. Lancet. 2012 Sep 29; 380(9848):1180–92. [PubMed: 23021287]

McAndrews MP, Cohn M. Neuropsychology in temporal lobe epilepsy: influences from cognitive neuroscience and functional neuroimaging. Epilepsy Res Treat. 2012; 2012:925238. [PubMed: 22957249]

McCormick C, Quraan M, Cohn M, Valiante TA, McAndrews MP. Default mode network connectivity indicates episodic memory capacity in mesial temporal lobe epilepsy. Epilepsia. 2013; 54(5):809–818. [PubMed: 23360362]

Mevel K, Landeau B, Fouquet M, La Joie R, Villain N, Mézenge F, Perrotin A, Eustache F, Desgranges B, Chételat G. Age effect on the default mode network, inner thoughts, and cognitive abilities. Neurobiol Aging. 2013; 34(4):1292–1301. [PubMed: 23084083]

Newman MEJ. The structure and function of complex networks. SIAM Review. 2003; 45:167–256.

Niu H, Li Z, Liao X, Wang J, Zhao T, Shu N, Zhao X, He Y. Test-retest reliability of graph metrics in functional brain networks: a resting-state fNIRS study. PLoS One. 2013; 8(9):e72425. [PubMed: 24039763]

Persson J, Lustig C, Nelson JK, Reuter-Lorenz PA. Age differences in deactivation: a link to cognitive control? J Cogn Neurosci. 2007; 19(6):1021–1032. [PubMed: 17536972]

Peterburs J, Thürling M, Rustemeier M, Göricke S, Suchan B, Timmann D, Bellebaum C. A cerebellar role in performance monitoring - evidence from EEG and voxel-based morphometry in patients with cerebellar degenerative disease. Neuropsychologia. 2015; 68:139–147. [PubMed: 25592368]

Power JD, Cohen AL, Nelson SM, Wig GS, Barnes KA, Church JA, Vogel AC, Laumann TO, Miezin FM, Schlaggar BL, Petersen SE. Functional network organization of the human brain. Neuron. 2011; 72(4):665–678. [PubMed: 22099467]

Quiske A, Helmstaedter C, Lux S, Elger CE. Depression in patients with temporal lobe epilepsy is related to mesial temporal sclerosis. Epilepsy Res. 2000; 39(2):121–125. [PubMed: 10759300]

Specht U, May T, Schulz R, Rohde M, Ebner A, Schmidt RC, Schütz M, Wolf P. Cerebellar atrophy and prognosis after temporal lobe resection. J Neurol Neurosurg Psychiatry. 1997; 62(5):501–506. [PubMed: 9153610]

Sporns O, Honey CJ, Kötter R. Identification and classification of hubs in brain networks. PLoS One. 2007; 2(10)

Song J, Nair VA, Gaggl W, Prabhakaran V. Disrupted Brain Functional Organization in Epilepsy Revealed by Graph Theory Analysis. Brain Connect. 2015 Epub ahead of print.

Song J, Desphande AS, Meier TB, Tudorascu DL, Vergun S, Nair VA, Biswal BB, Meyerand ME, Birn RM, Bellec P, Prabhakaran V. Age-related differences in test-retest reliability in resting-state brain functional connectivity. PLoS One. 2012; 7(12):e49847. [PubMed: 23227153]

Wang JH, Zuo XN, Gohel S, Milham MP, Biswal BB, He Y. Graph theoretical analysis of functional brain networks: test-retest evaluation on short- and long-term resting-state functional MRI data. PLoS One. 2011; 6(7):e21976. [PubMed: 21818285]

Wang J, Zuo X, He Y. Graph-based network analysis of resting-state functional MRI. Front Syst Neurosci. 2010; 4:16. [PubMed: 20589099]

Zhao F, Kang H, You L, Rastogi P, Venkatesh D, Chandra M. Neuropsychological deficits in temporal lobe epilepsy: A comprehensive review. Ann Indian Acad Neurol. 2014; 17(4):374–382. [PubMed: 25506156]

Zeng H, Pizarro R, Nair VA, La C, Prabhakaran V. Alterations in regional homogeneity of resting-state brain activity in mesial temporal lobe epilepsy. Epilepsia. 2013; 54(4):658–666. [PubMed: 23294137]

Zhang X, Tokoglu F, Negishi M, Arora J, Winstanley S, Spencer DD, Constable RT. Social network theory applied to resting-state fMRI connectivity data in the identification of epilepsy networks with iterative feature selection. J Neurosci Methods. 2011; 199(1):129–139. [PubMed: 21570425]

Appendix

Global efficiency is defined as:

$$E_{Global}(G)=\frac{1}{N(N-1)\sum_{i\neq j\in G}\frac{1}{d_{ij}}}$$

where G is the graph, N is the number of nodes, and d is the shortest path length between nodes i and j. The shortest path is the minimum number of connections needed to link one node to another.

The local efficiency is defined as:

$$E_{Local}(G)=\frac{1}{N}\sum_{i\in G}E_{Global}(G_i)$$

where $E_{Global}(G_i)$ is the global efficiency of node i is the subgraph composed of the neighbors of such node.

Both global and local efficiencies lie between 0 and 1, with a value of 0 indicating no efficiency and a value of 1 indicating full efficiency.

Highlights

- Patients showed higher global integration compared to controls.
- Patients showed lower global segregation compared to controls.
- Patients failed to engage most of DMN-related regions as hubs compared to controls.
- Patients engaged cerebellar regions as connector hubs.
- Using two differentially defined graphs synergistically contributed to findings.

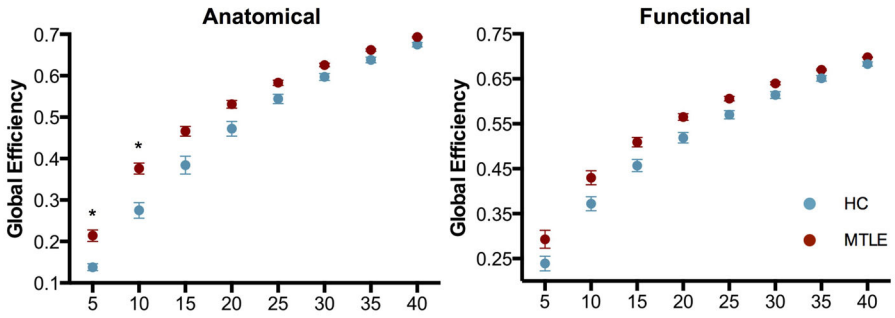

Figure 1. Global efficiency

Global efficiency in anatomically defined (left) and functionally defined (right) graphs across a range of network densities between mTLE (red) and healthy subjects (blue). Both kinds of networks show moderately higher global efficiency in patients compared to controls. * Significant at $p<0.05$, corrected for multiple comparisons.

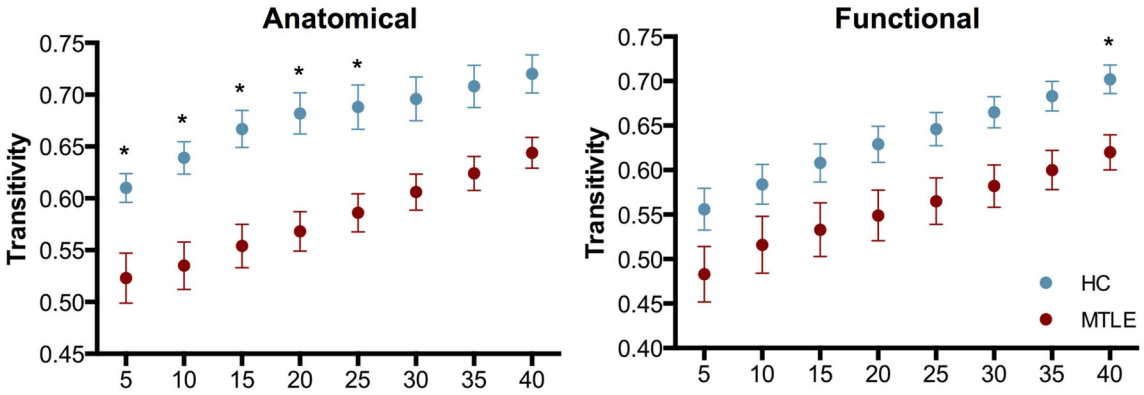

Figure 2. Global clustering

Global clustering in the anatomically defined (left) and the functionally defined (right) graphs across a range of network densities between mTLE (red) and healthy subjects (blue). In both kinds of networks, patients show lower global clustering when compared to controls. * Significant at $p<0.05$, corrected for multiple comparisons.

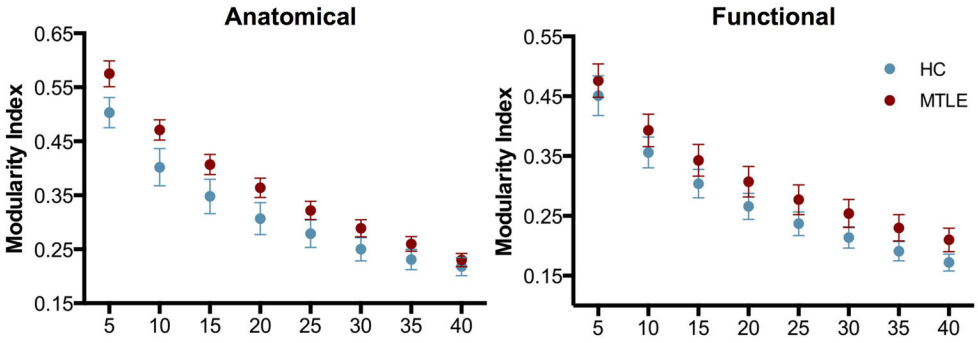

Figure 3. Modularity index

Modularity index in anatomically (left) and functionally defined (right) networks across a range of network densities between mTLE (red) and healthy subjects (blue). No significant differences were obtained at any density level.

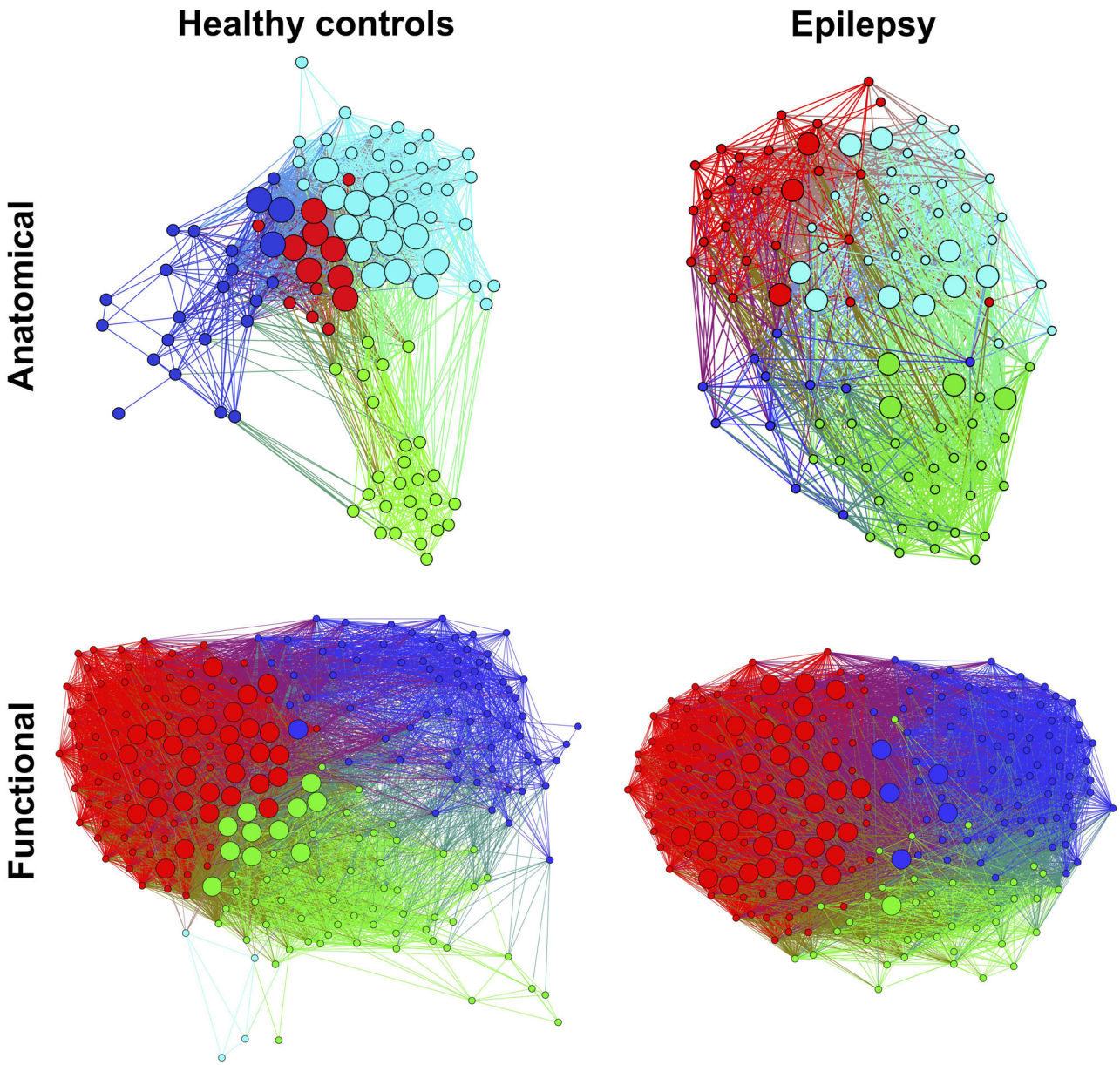

Figure 4. Local efficiency

Local efficiency in anatomically (top) and functionally defined (bottom) networks between mTLE (red) and healthy subjects (blue). Filled nodes are those that presented significant differences at FDR correction. Calculated at a density threshold of 37%.

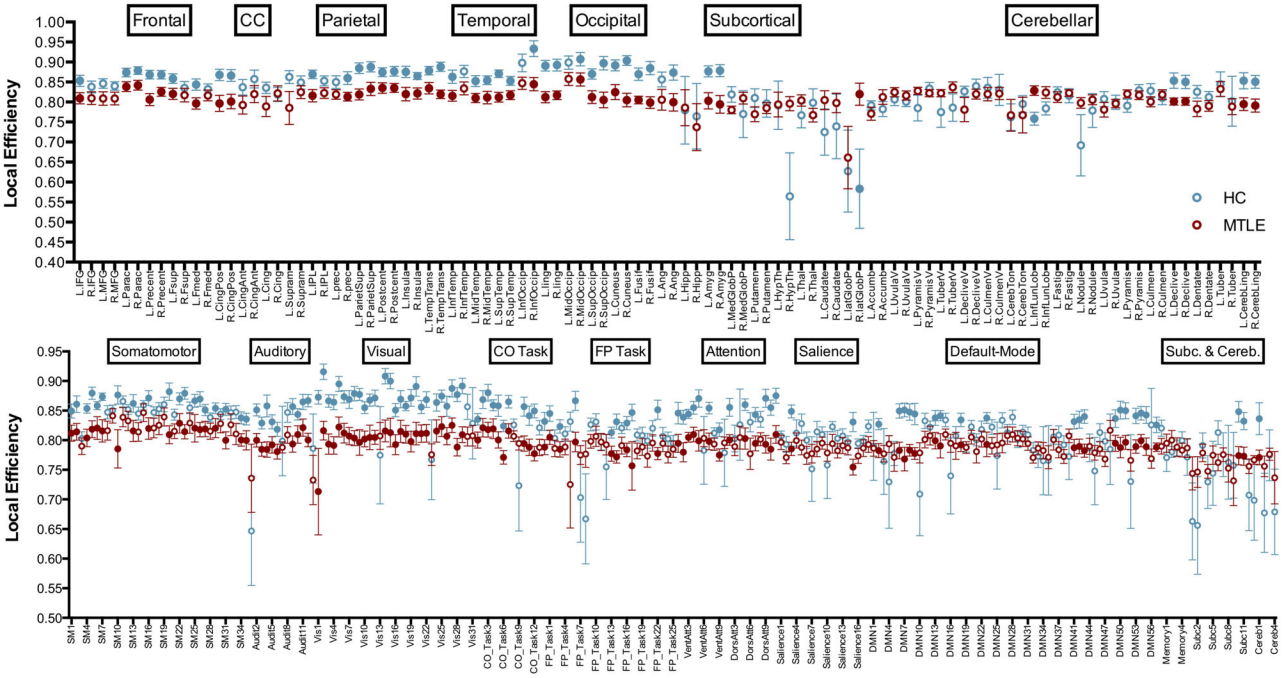

Figure 5. 2D visualization of modularity

Modularity in anatomically (top) and functionally defined (bottom) networks in HC (left) and mTLE (right). Hubs are represented as bigger spheres. Different colors represent different modules. Anatomically defined network: green= cerebellar regions; cyan= mainly parietal, temporal, and occipital regions; red=mainly frontal and parietal; blue=frontal, insular and subcortical in HC, only subcortical in mTLE. Functionally defined network: red=mostly SM, visual, attention, and task control; green=mainly task control, and salience in controls, and salience and subcortical areas in mTLE; cyan= cerebellar (in controls only); blue=mainly DMN. Nodes with stronger and higher number of connections are spatially closer while those with weaker and lower number of connections are farther in space. Calculated at a density threshold of 37%.

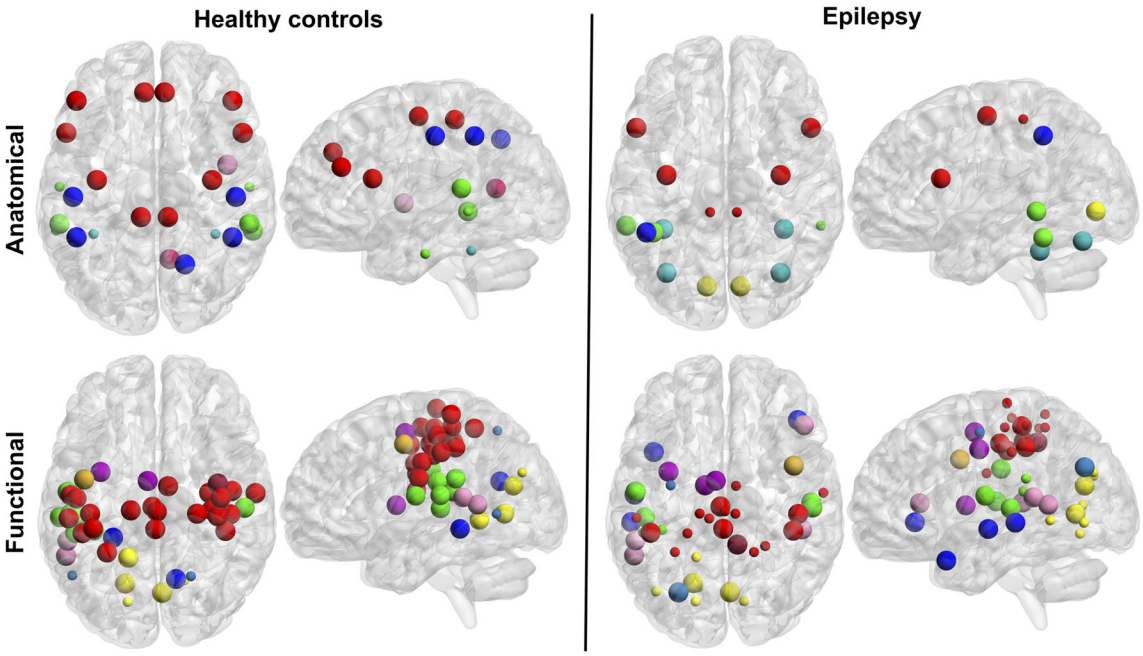

Figure 6. Functional hubs

Provincial (small spheres) and connector (bigger spheres) hubs of the anatomically defined (top) and the functionally defined (bottom) networks in healthy subjects (left) and patients with mTLE (right). Different colors represent different locations (anatomically defined) or different functional systems (functionally defined). Anatomically defined network: red=frontal; blue=parietal; green=temporal; yellow=occipital; cyan=cerebellar; pink=insular; magenta=cingulate cortex. Functionally defined network: red=somatomotor; green=auditory; blue=DMN; pink=ventral attention; magenta=cingulo-opercular task control; yellow=visual; brown=salience; orange=fronto-parietal task control; teal=dorsal attention. Calculated at a density threshold of 37%.

Table I

Clinical and demographic characteristics of the patient group

Patients	Age	Gender	SO (years)	H	No. AEDs
1	43	F	19	L	3
2	34	F	1	L	2
3	40	M	32	L	3
4	52	F	49	L	6
5	26	F	25	L	3
6	36	F	31	R	2
7	29	F	14	L	2
8	53	M	16	R	3
9	43	F	35	L	2
10	19	F	2	L	3
11	27	F	3	R	2

H: hemisphere; SO: syndrome onset; AED: antiepileptic drug.

Epilepsy Res. Author manuscript; available in PMC 2017 July 01.

Table II

Summary of characteristics for patients and control subjects

	mTLE (*n*=11)	**HC (*n*=15)**
Age (mean ± SD)	36.5 ± 10.9	36.8 ± 14.0
Gender (M/F)	2/9	7/8
Syndrome Onset (mean ± SD)	20.6 ± 15.4	-
Number of AED (mean ± SD)	2.8 ± 1.2	-
HS location (L/R)	8/3	-

HS: hippocampal sclerosis; AED: antiepileptic drugs.